

Effect of Temperature on the Dispersion Properties of Polypropylene Fibers

A. E. Belal,¹ A. A. Hamza,² T. Z. N. Sokkar,² M. A. El-Bakary,² K. M. Yassien¹

¹Physics Department, Faculty of Science, Aswan, South Valley University, Egypt

²Physics Department, Faculty of Science, Mansoura University, Mansoura 35516, Egypt

Received 11 June 2004; accepted 10 January 2005

DOI 10.1002/app.22100

Published online in Wiley InterScience (www.interscience.wiley.com).

ABSTRACT: A Biolar PI polarizing interference microscope (a Pluta microscope) attached to a special hot stage was used to study the influence of temperature on the dispersion properties of polypropylene fibers with different deniers (6 D and 90 mm, 6 D and 150 mm, and 12 D and 150 mm) over the temperature range of 30–50°C. This study was carried out with a variable-wavelength interferometry technique. Constant A of Cauchy's dispersion formula and the

oscillation and dispersion energies for light vibrating parallel and perpendicularly to the fiber axis were determined at different temperatures. Microinterferograms are given for illustration. © 2005 Wiley Periodicals, Inc. *J Appl Polym Sci* 98: 1135–1141, 2005

Key words: dispersions; refractive index; poly(propylene) (PP)

INTRODUCTION

Interferometry is a very useful tool in fiber science. It provides quantitative information about the optical properties of fibers and the variation of these properties along the axis of fibers.^{1–4} The range and detail of structural information provided by interferometric methods are of great potential importance in quality control in the textile industry.

A specific microinterferometric technique called *variable-wavelength interferometry* (VAWI) is recommended for measuring the spectral dispersion for the refractive indices of textile fibers.^{5,6} This technique uses monochromatic light with a variable wavelength (λ). The VAWI technique includes VAWI-1, which is suitable for studying fibers that produce a high optical path difference ($\delta > 3\lambda$). Also, it includes an ultraprecise object-adopted version [adaptive variable-wavelength interferometry (AVAWI)],⁷ which is suitable for studying samples that produce a small optical path difference ($\delta < 3\lambda$). The only directly measured parameters are the interfering spacing (b) and the fiber thickness, whereas other quantities are observed and read from the calibration graph $b(\lambda)$.⁷

The VAWI technique was applied for measuring the optical parameters of fibers.^{6,8,9} Hamza et al.⁹ derived a mathematical formula to determine the spectral dispersion curve of a fiber, considering the cross-sectional area and area enclosed under the fringe shift,

with the VAWI technique. The refractive index is a function not only of the wavelength but also of the temperature, chemical composition, and physical state of the matter. The changes in the refractive index with the temperature are called *temperature dispersions*.¹⁰

Faust¹¹ designed an optothermal device to study the variation of the refractive index of the fiber with the variation of that of the surrounding liquid via changes in the temperature of the interferometric system. Hamza et al.¹² studied the effect of temperature (within 15–31°C) on the optical properties of wool fibers. Recently, Hamza et al.¹³ designed a hot stage attached to a multiple-beam Fizeau interferometric system to study the optical and structural properties of fibers.

In this work, we studied the influence of temperature on the spectral dispersion curves of refractive indices n^{\parallel} and n^{\perp} for polypropylene (PP) fibers with different deniers (6 D and 90 mm, 6 D and 150 mm, and 12 D and 150 mm) with the VAWI technique. These studies were carried with a constructed hot stage¹⁴ for heating the fiber attached to the Biolar PI double-refracting interference microscope. Constant A of Cauchy's dispersion formula and the oscillation and dispersion energies for light vibrating parallel and perpendicularly to the fiber axis (E_o^{\parallel} , E_o^{\perp} , E_d^{\parallel} , and E_d^{\perp} , respectively) were provided at different temperatures.

THEORETICAL CONSIDERATIONS: MEASUREMENT OF THE SPECTRAL DISPERSION OF N^{\parallel} AND N^{\perp}

When a transparent object is placed in the object plane of a light-transmitting interferometer, an optical path

Correspondence to: A. A. Hamza (hamzaaa@mans.edu.eg).

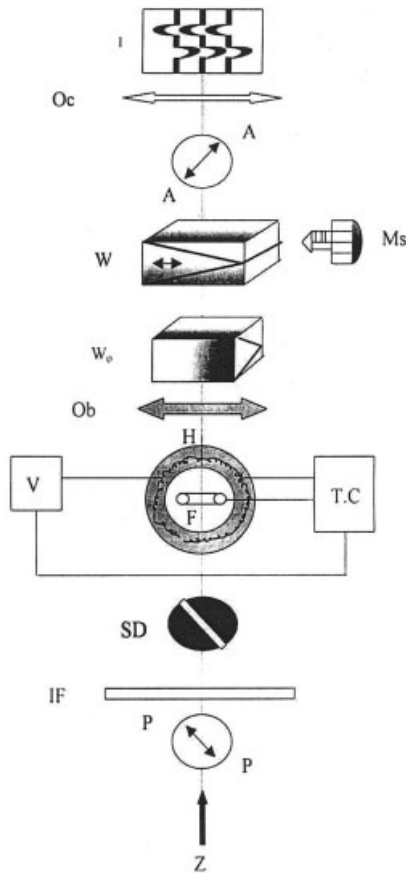


Figure 1 Schematic diagram of the double-refracting interference system applied to the VAWI technique⁶ (Z = source of light; IF = interference filter; P = polarizer; SD = slit diaphragm; H = hot stage; F = fiber under study; Ob = objective lens; W and W_o = Wollaston prisms; A = analyzer; Ms = micrometer screw; Oc = ocular; I = microinterferogram).

difference (δ) is obtained between the light rays passing through the object and the surrounding medium. If the refractive index of this object is n , its thickness is t , and the surrounding medium refractive index is n' , the optical path difference (δ_s) is given by the following general equation:⁶

$$\delta_s = (n_{is} - n_s')t = (m_1 + q_s)\lambda_s \quad (1)$$

where index i denotes the light vibration parallel (\parallel) or perpendicular (\perp) to the fiber axis; s is the coincidence number; and λ is the wavelength of the light used, which continuously varies in the visible region of the spectrum. The coincidence positions are at $\lambda_1, \lambda_2 \dots \lambda_s$. q_s , an arbitrary integer, takes the values 1, 2, 3 ..., and q_1 is 0 (first coincidence). m_1 is the initial interference order and is given by the following equation:⁶

$$m_1 = q_s \frac{b_s}{b_1 - b_s} \quad (2)$$

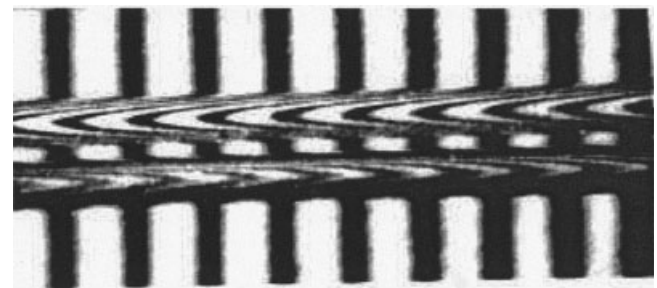
where b_s is the interfering spacing that corresponds to λ_s .

For AVAWI in the domain of b , eq. (2) can be written in the following form, where b_1 is the interference spacing corresponding to λ_1 :

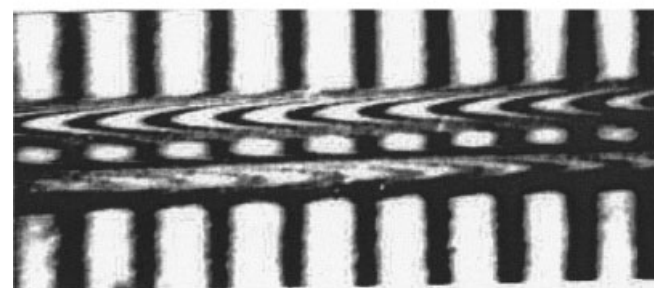
$$(m_1 + q_s)b_s = m_1b_1 \quad (3)$$

Therefore, we take the average quantity $\overline{m_s b_s}$, which is defined as⁶

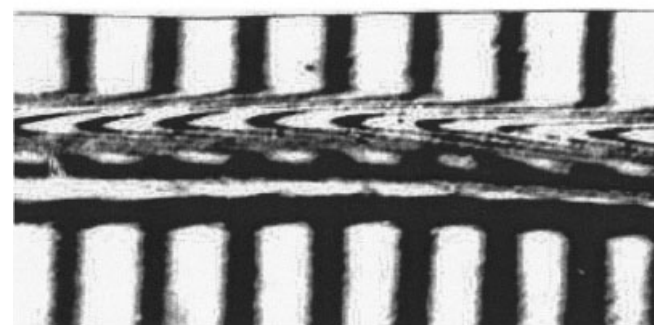
$$\overline{m_s b_s} = \frac{\sum_{s=1}^s (m_1 + q_s)b_s}{s} = C \quad (4)$$



(a)

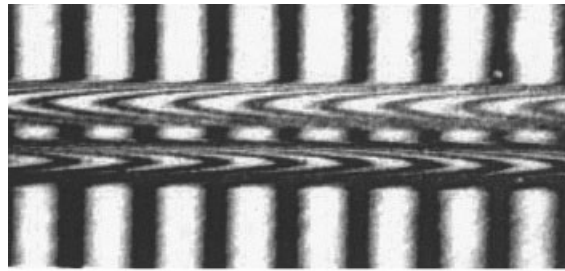


(b)

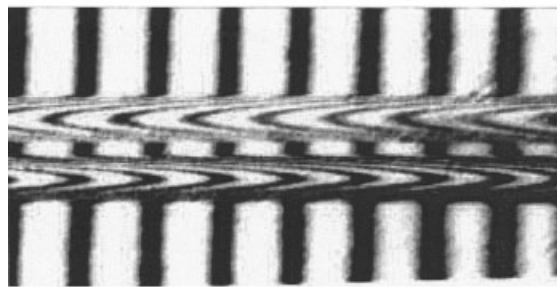


(c)

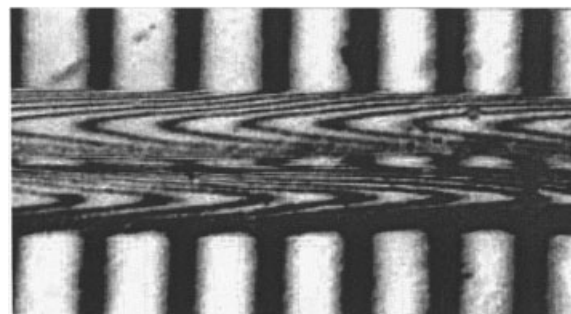
Figure 2 Microinterferograms of coincidence positions of n^{\parallel} of PP fiber (6 D and 90 mm) at different temperatures: (a) 34, (b) 39, and (c) 47°C.



(a)



(b)



(c)

Figure 3 Microinterferograms of coincidence positions of n^\perp of PP fiber (6 D and 150 mm) at different temperatures: (a) 30, (b) 35, and (c) 45°C.

where m_s is equal to $m_1 + q_s$ and C is the mean fringe displacement. δ_s can be determined with AVAWI (b) with the following relation:⁶

$$\delta_s = C \frac{\lambda_s}{b_s} \quad (5)$$

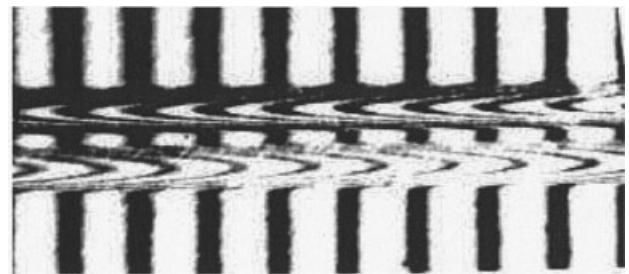
With eqs. (1), (2), (4), and (5), the spectral dispersion curves of refractive indices can be determined.

EXPERIMENTAL

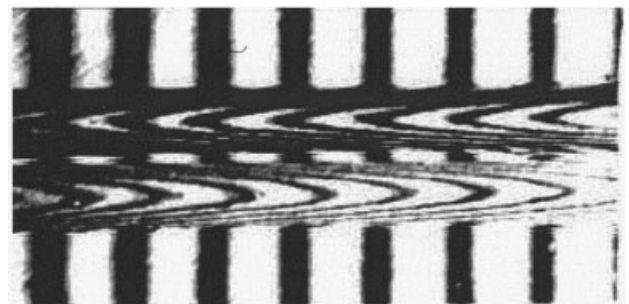
A hot stage¹⁴ (Fig. 1) attached to a Biolar PI double-beam interference microscope was used to study the

influence of temperature on the spectral dispersion curves of n^\parallel and n^\perp of PP fibers with different deniers (6 D and 90 mm, 6 D and 150 mm, and 12 D and 150 mm).

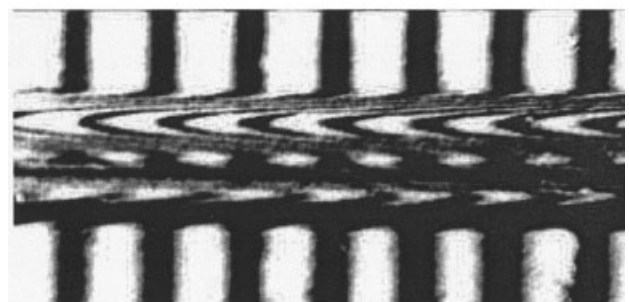
The fiber under study was fixed with a suitable adhesive material to a glass microscope slide. For PP fibers, the whole fringe shift was not observable in the field of the microscope when a fiber was used without an immersion liquid. Therefore, an immersion liquid of a medium refractive index was used to minimize



(a)



(b)



(c)

Figure 4 Microinterferograms of coincidence positions of n^\parallel of PP fiber (12 D and 150 mm) at different temperatures: (a) 30, (b) 35, and (c) 45°C.

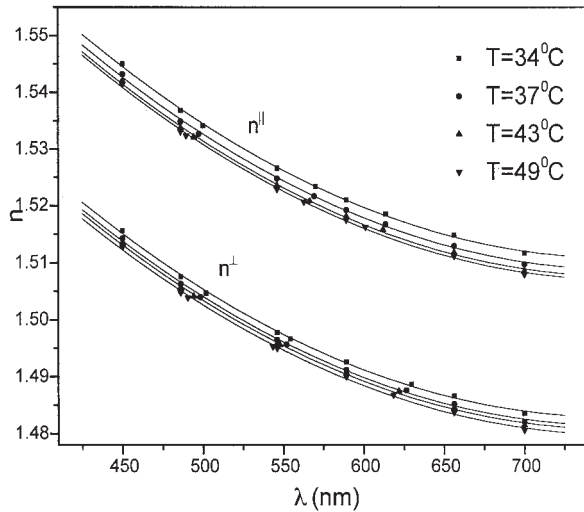


Figure 5 Spectral dispersion curves of n^{\parallel} and n^{\perp} for PP fiber (6 D and 90 mm) at different temperatures with the VAWI technique.

the fringe displacement ($m_s b_s$) observed in the field of the microscope. A drop of liquid was placed on the fixed fiber, and then a covering glass was placed on it. The refractive indices of the immersion liquids were 1.6165 (6 D and 90 mm) and 1.6356 (6 D and 150 mm, 12 D and 150 mm) at 30°C. The thermal coefficients of the immersion liquids were measured to be -4.3×10^{-4} and $-4.5 \times 10^{-4} \text{ } ^\circ\text{C}^{-1}$, respectively.

The objective double-refracting prism was adjusted to be in a crossed position with the main Wollaston prism. The hot stage in which the fiber was fixed was placed on the microscope stage, as shown in Figure 1. The interference image of the fiber had two images, one when monochromatic light vibrating parallel to the fiber axis was used and the other for the perpendicular direction. The contrast of the fringes and the intensity of the interference field were optimized by the adjustment of the width of the condenser slits. This slit cooperated well with the wedge interference filter (continuous-wavelength interference filter) and reduced a possible aperture error in the measurement of the optical path difference. The interference filter was located as near as possible to the slit.

RESULTS AND DISCUSSION

By the movement of the interference filter from the red region to the blue region of the visible range (with the wavelength of light varied), the coincidence and anti-coincidence of the fringe with the medium fringe were obtained.⁶

Figures 2–4 present microinterferograms showing the coincidence positions for the fringe shifts of PP fibers (6 D and 90 mm, 6 D and 150 mm, and 12 D

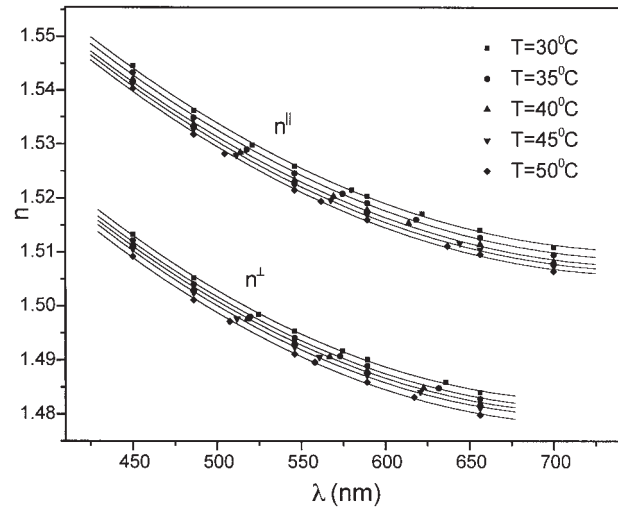


Figure 6 Spectral dispersion curves of n^{\parallel} and n^{\perp} for PP fiber (6 D and 150 mm) at different temperatures with the VAWI technique.

and 150 mm, respectively) at different temperatures. From these microinterferograms, it is obvious that when the temperature of the system increases from room temperature to any elevated temperature, the fringe shifts change in both directions, so the coincidence also must be changed. To obtain this coincidence again, we move the interference filter; the wavelength is changed, so b is changed. The values of b are measured at these coincidences with the micrometer screw linked to the main double-refracting prism, as shown in Figure 1. The Biolar PI microinterferometer enables wavelength λ of monochromatic light to be measured in real time because there is a constant relation between b and the wave-

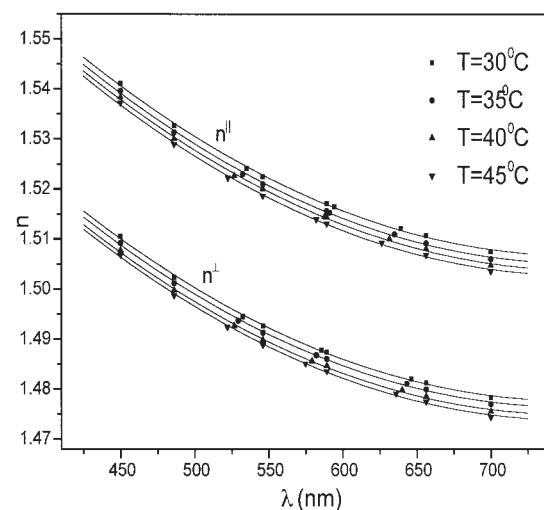


Figure 7 Spectral dispersion curves of n^{\parallel} and n^{\perp} for PP fiber (12 D and 150 mm) at different temperatures with the VAWI technique.

TABLE I
Dispersion and Oscillation Energies of Three Different Samples of PP Fibers for Light Vibrating Parallel and Perpendicularly to the Fiber Axis at Different Temperatures (T')

PP (6 D, 90 mm)					PP (6 D, 150 mm)					PP (12D, 150 mm)				
$T(^{\circ}\text{C})$	E_d^{\parallel}	E_o^{\parallel}	E_d^{\perp}	E_o^{\perp}	$T(^{\circ}\text{C})$	E_d^{\parallel}	E_o^{\parallel}	E_d^{\perp}	E_o^{\perp}	$T(^{\circ}\text{C})$	E_d^{\parallel}	E_o^{\parallel}	E_d^{\perp}	E_o^{\perp}
29	9.24	7.56	8.58	7.52	30	9.16	7.52	8.49	7.49	30	9.07	7.50	8.42	7.48
34	9.18	7.54	8.53	7.51	35	9.11	7.50	8.43	7.46	35	9.02	7.49	8.38	7.47
39	9.14	7.53	8.52	7.50	40	9.08	7.49	8.41	7.45	40	9.00	7.48	8.33	7.46
45	9.12	7.52	8.50	7.49	45	9.04	7.48	8.38	7.44	45	8.96	7.47	8.29	7.44
					50	9.00	7.46	8.34	7.43					

length of the light entering the optical system of the microscope.⁶ This relationship between b and λ is considered as the basic calibration graph $b(\lambda)$. The calibration procedure¹⁵ was carried out very carefully with a He-Ne laser beam. The setup for the microinterferometer calibration process and the calibration curve $b(\lambda)$ of the Biolar PI double-refracting interference microscope were given.⁹ The interference order was measured from eq. (2), and then the average of the calculated m_1 values was taken. Then, the spectral dispersion curves of n^{\parallel} and n^{\perp} were calculated with eqs. (1), (4), and (5) with respect to $m_1 \pm 1$. The dispersion of the immersion liquids was determined with an Abbe refractometer and was extrapolated with Cauchy's formula. The dispersion of the liquids was taken into consideration during the calculation of the dispersion parameters of the fibers.

Figures 5–7 give the spectral dispersion curves of the refractive index for the samples at different temperatures. The refractive index varies with the variation of the wavelength of the incident light beam. This variation is due to the interaction between light and

matter, which leads to refraction effects, which are essentially forced vibrations of electrons with natural wavelength λ_n by an oscillatory electric field of wavelength λ .¹⁶ All the samples of PP fibers had normal dispersion curves in the range of the visible spectrum at different temperatures because the refractive index for all the samples decreased as the wavelength of light increased.

Also, Figures 5–7 show that the spectral dispersion values of the samples decreased as the temperature increased. This is due to the fact that the temperature is an important operator that affects the dispersion properties of PP fibers. The study of the optical properties of fibers at different temperatures throws light on the optothermal behavior of the investigated fibers. At low temperatures, most plastics become hard and brittle, whereas at high temperatures, they are rubbery or leathery and have great flexibility and toughness.^{17,18} From the spectral dispersion curves $[n(\lambda)]$ of the PP fibers, we can read out n for any wavelength λ at any elevated temperature.

Constant A of Cauchy's dispersion formula can be calculated with the following equation:¹⁹

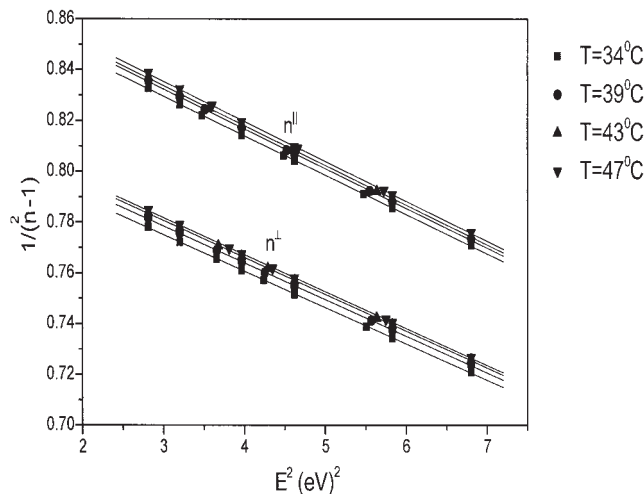


Figure 8 Relation between $1/(n^2 - 1)$ for light vibrating parallel and perpendicularly to the fiber axes and E^2 at different temperatures for PP fiber (6 D and 90 mm).

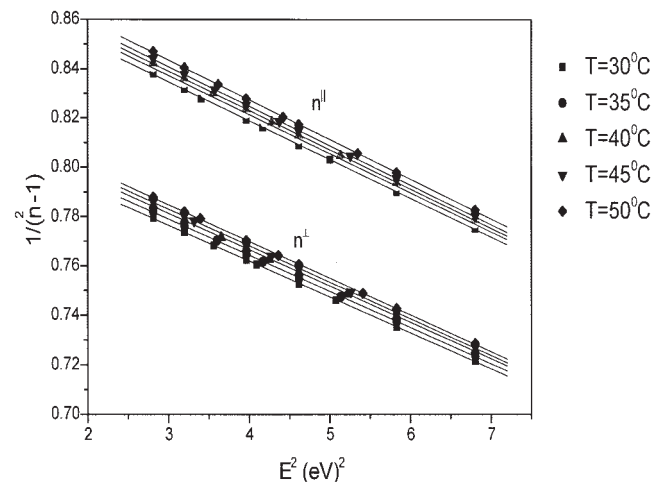


Figure 9 Relation between $1/(n^2 - 1)$ for light vibrating parallel and perpendicularly to the fiber axes and E^2 at different temperatures for PP fiber (6 D and 150 mm).

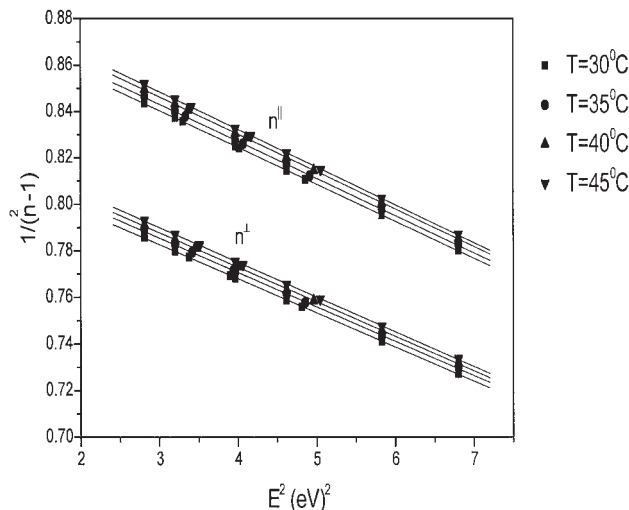


Figure 10 Relation between $1/(n^2 - 1)$ for light vibrating parallel and perpendicularly to the fiber axes and E^2 at different temperatures for PP fiber (12 D and 150 mm).

$$n = A + \frac{B}{\lambda^2} + \frac{C}{\lambda^4} + \dots \quad (6)$$

This formula contains three (or even more) constants, A , B , and C , characterizing the medium of concern. These constants are usually determined experimentally by the measurement of n for three different values of λ . For many practical purposes, it is sufficient to consider only the first two terms of eq. (6). By plotting the relation between n and $1/\lambda^2$ at different temperatures, we obtain a straight line; its intercept on the vertical axis is constant A . This constant for light vibrating parallel and perpendicularly to the fiber axis (A^{\parallel} and A^{\perp}) was determined for the samples at different temperatures, and the results are given in Table I. As the temperature increased, constants A^{\parallel} and A^{\perp} decreased for all samples.

The dispersion energy (E_d) plays an important role in determining the behavior of refractive indices and properly normalizes the interaction potential describing these optical effects.²⁰ The following equation is proposed to express n including electronic and lattice

contributions at short wavelengths, whose lattice term may be neglected:²¹

$$(n^2 - 1)^{-1} = \frac{E_o}{E_d} - \frac{E^2}{E_d E_o} \quad (7)$$

where E_o is the average energy gap or oscillation energy, E is the photon energy, and n is the refractive index of the material. This equation can be used for light vibrating parallel or perpendicularly to the fiber axis. The plot of $(n^2 - 1)^{-1}$ versus E^2 approaches a straight line, its intercept on the vertical axis is the ratio E_o/E_d , and the slope is $1/E_o E_d$. Figures 8–10 show the relation between $1/(n^2 - 1)$ and E^2 for light vibrating parallel and perpendicularly to the fiber axis at different temperatures for the samples. From these figures, the energies E_o and E_d can be determined at different temperatures with both the slope and intercept of the fitted straight line. The results for E_o^{\parallel} , E_o^{\perp} , E_d^{\parallel} , and E_d^{\perp} at different temperatures are given in Table II for the samples. E_o^{\parallel} , E_o^{\perp} , E_d^{\parallel} , and E_d^{\perp} nearly decreased as the temperature increased for different samples of PP fibers. The results show that the structure of PP fibers depends on the thermal properties, which have a direct effect on optical and structural parameters, such as n , E_o , and E_d .

CONCLUSIONS

A hot stage¹⁴ attached to a Biolar PI double-refracting interference microscope is a good technique for studying the optothermal behavior of fibers. The study of the influence of temperature on the dispersion properties of the fibers under study shows that, when the temperature rises, the spectral dispersion curves of the samples have lower refractive indices. Also, the results show that the samples have normal dispersions at different temperatures. From the dispersion curves, we can read out n of any wavelength λ at any elevated temperature.

With the spectral dispersion curves, A^{\parallel} , A^{\perp} , E_o^{\parallel} , E_o^{\perp} , E_d^{\parallel} , and E_d^{\perp} can be determined at different temperatures. The results show that these values nearly de-

TABLE II
Cauchy's Constants for Three Different Samples of PP Fibers for Light Vibrating Parallel and Perpendicularly to the Fiber Axis at Different Temperatures (T_s)

PP (6 D, 90 mm)			PP (6 D, 150 mm)			PP (12 D, 150 mm)		
T (°C)	A^{\parallel}	A^{\perp}	T (°C)	A^{\parallel}	A^{\perp}	T (°C)	A^{\parallel}	A^{\perp}
29	1.487	1.460	30	1.486	1.457	30	1.483	1.454
34	1.486	1.458	35	1.484	1.456	35	1.481	1.453
39	1.484	1.457	40	1.483	1.455	40	1.480	1.452
45	1.483	1.457	45	1.482	1.454	45	1.479	1.450
			50	1.482	1.452			

crease as the temperature increases. Also, these values show the same behavior as the refractive index with the temperature.

References

1. Hamza, A. A. *J Microsc* 1986, 142, 35.
2. Barakat, N. *Text Res J* 1971, 41, 67.
3. Pluta, M. *J Microsc* 1972, 96, 309.
4. Barakat, N.; Hamza, A. A. *Interferometry of Fibrous Materials*; Adam Hilger: Bristol, NY, 1990.
5. Pluta, M. *Opt Appl* 1985, 15, 375.
6. Pluta, M. *J Microsc* 1988, 149, 97.
7. Pluta, M. *J Microsc* 1987, 145, 191.
8. Hamza, A. A.; Sokkar, T. Z. N.; El-Bakary, M. A. *J Opt A* 2002, 3, 421.
9. Hamza, A. A.; Fouda, I. M.; Sokkar, T. Z. N.; El-Bakary, M. A. *J Opt A* 1999, 1, 359.
10. Jurgen, R. Meyer-Arendt *Introduction to Classical and Modern Optics*; Prentice-Hall, Inc., Englewood Cliffs, N.J., 1972; p 57.
11. Faust, R. C. *Proc Phys Soc London Sect B* 1954, 67, 138.
12. Hamza, A. A.; Fouda, I. M.; El-Farahaty, K. A.; El-Sayed, K. A. *Acta Phys Pol A* 1988, 73, 767.
13. Hamza, A. A.; Sokkar, T. Z. N.; El-Farahaty, K. A.; El-Dessoky, H. M. *J Phys: Condens Matter* 1999, 11, 5331.
14. Belal, A. E.; Hamza, A. A.; Sokkar, T. Z. N.; El-Farahaty, K. A.; Yassien, K. M. *Polym Test* 2002, 21, 877.
15. Pluta, M. *Opt Appl* 1990, 20, 259.
16. Pluta, M. *Advanced Light Microscopy*; PWN: Warsaw, 1993; Vol. 3.
17. Tager, A. *Physical Chemistry of Polymers*; Mir: Moscow, 1978.
18. Shengmei, Y.; Roger, E. M. *Plasma Deposition of Polymeric Thin Films*; Wiley: New York, 1994; p 77.
19. Pluta, M. *Advanced Light Microscopy*; Polish Scientific: Warsaw, 1988; Vol. 1, p 1988.
20. Wemple, S. H.; Didomenico, M. *J Phys Rev B* 1971, 3, 1338.
21. Wemple, S. H. *Appl Opt* 1979, 18, 31.